IJPSR (2020), Volume 11, Issue 11 (Research Article)

INTERNATIONAL JOURNAL OF PHARMACEUTICAL SCIENCES AND RESEARCH

Received on 18 October 2019; received in revised form, 20 September 2020; accepted, 22 September 2020; published 01 November 2020

INCREASED PROPERTIES AND CITOCOMPATIBILITY OF ZINC OXIDE-MAGNESIUM CEMENT

Giseli C. Paula [1], Adriano Trajano [2], Ana D. Pinzón-García [3], Rubén D. Sinisterra [3] and Maria E. Cortes [*1]

Universidade Federal de Minas Gerais, Faculty of Dentistry [1], Restorative Dentistry Department, Universidade Federal de Minas Gerais, Mechanical Engineering [2], Universidade Federal de Minas Gerais, Institute of Exact Science [3], Chemistry Department, Belo Horizonte, Minas Gerais, Brazil. Av. Antônio Carlos, 6627, Pampulha, 31270-901, Belo Horizonte, MG, Brazil.

Keywords:

Chemical preparation, Nanocomposites, Chemical properties, Nano-hydroxyapatite

Correspondence to Author:
Professor Maria Esperanza Cortés

Universidade Federal de Minas Gerais, Faculty of Dentistry, Restorative Dentistry Department, Belo Horizonte, Minas Gerais, Brazil. Av. Antônio Carlos, 6627, Pampulha, 31270-901, Belo Horizonte, MG, Brazil.

E-mail: mecortes@ufmg.br

ABSTRACT: Zinc oxide-magnesium has been used in dentistry with limitations especially related to its high acidity and low biocompatibility. The objective of this study was to develop cement based on nano-hydroxyapatite (nHA), chitosan as more biocompatibility agents to increase zinc oxide-magnesium cito-compatibility. The formulations prepared were: 1. Complete cement (HCP) with nHA, zinc oxide-magnesium, and chitosan; 2. cement without nHA (CP); 3. Without chitosan (HP); 4. Without zinc oxide-magnesium (HC), and CPZn as control. All cement were compared for setting times, solubility, contact angle, pH, calcium ion release, shear strength, the thermogravimetry analysis, X-ray diffraction, Raman spectroscopy, 3T3-L1 fibroblasts cell compatibility, and antimicrobial activity. The results showed that HCP cement had setting time (mean ± S.D) of 5.5 ± 0.18 min, ($p \geq 0.05$) and neutral pH values on 14 days, calcium release of 10 mgL^{-1}, and solubility with a value of 2.15%. The physicochemical characterization showed an expected pattern from the raw materials and composition. The values of the contact angle measurements indicated increased wettability for the HCP than the control cement. The zinc oxide-magnesium presence was important to improve the mechanical strength. HCP and HC cement had similar fibroblast compatibility and significantly higher than the others ($p \leq 0.05$). The experimental cement showed antimicrobial activity against *P.g, F.n, A.a,* and *S.a*on the diffusion agar test higher than control cement (17.6 ± 1.1 mm) $p \leq 0.05$. These studies indicated that this cement showed appropriate physicochemical properties with high cytocompatibility, maintaining its resistance and antimicrobial action, suggesting be beneficial in dentistry.

INTRODUCTION: New materials that seek better performance on wet dental surfaces are being continuously introduced in the market to optimize care for dental patients, especially in the protection of pulp injuries [1].

QUICK RESPONSE CODE

DOI: 10.13040/IJPSR.0975-8232.11(11).5484-96

This article can be accessed online on www.ijpsr.com

DOI link: http://dx.doi.org/10.13040/IJPSR.0975-8232.11(11).5484-96

Ideal dental cement must be inert to the oral cavity, must have good strength, have some dimensional stability, should reduce the penetration of oral fluids and the postoperative sensitivity, must not have acidic pH [2], serve as a barrier against the passage of irritating agents from other restorative materials, including helping to avoid the injury to dentin-pulp complex [3].

Several cements are commercially available for use as luting agents, and among them, calcium hydroxide, mineral trioxide aggregate (MTA), and calcium silicate are widely used due to its ability to

stimulate pulp repair, dentin bridge formation, and its antimicrobial activity due from the high pH generated by the material [2-6]. However, calcium hydroxide-based cement shows several limitations, including rapid degradation, which is often incompatible with the repair time, the formation of tunnel defects in the dentin bridge, intense caustic, and inadequate sealing [7, 8]. Despite the high clinical efficacy of MTA and calcium silicate cement, there were also some issues that prevented the clinicians from using it for many cases. The major ones being very long setting time and difficult manipulation [6]. Thus, allowing microleakage of contaminants is buffering rapidly by the fluid of dentinal tubules, low mechanical resistance, and lack of adhesion to dental structures [9].

The Zinc phosphate cement belongs to the class of materials known as acid-base cement. It is widely used in dentistry for several uses such as luting or lining, for pulp protection under restoration of metal or plastic, and for fixation of crowns, bridges, inlays. Its main compound is zinc oxide, considered as the solid phase of cement, and it is usually mixed with small quantities of MgO, which favors the deactivation of zinc oxide particles in the sintering step. As a consequence, this process leads to a retarding of the setting reaction of the cement and a liquid phase, which contains phosphoric acid and water [10, 11], which brings an acidic pH to the medium and to exhibit an exothermic reaction. This cement can damage the pulp tissues that remain in contact with the cement; it is not a good choice for clinical applications [12].

The nano-hydroxyapatite (nHA), has been used effectively in medical and dental applications rates due to its high biocompatibility and bioactivity. It benefits the development of bone tissue and the formation of a strong bond between the surface of the nHA and the tissue; therefore, it may be a safe alternative for pulp repair as it has a similar chemical structure as a human tooth made of apatite [11, 13] while the bioactivity of nHA favors the formation of dentin by the deposition of a superficial layer of apatite in the presence of pulp fluids. This deposition assists maintain the integrity of the pulp tissue and induce a faster and more efficient formation of dentin [3]. Nevertheless, significant disadvantages of nano-hydroxyapatite are its brittleness, low tensile strength, and moldability, which are essential properties for dental cement [12], and the sintered process decreases the nanostructured properties, reducing its chemical activity and reabsorption properties when in a biological environment [14].

Currently, the use of natural polymers has been given increasing interest due to some of their unique properties, such as non-toxicity, degradability, and favorable biocompatibility. The chitosan is a hydrophilic biopolymer that is low cost, helpsto maintain the moisture of the environment and biodegradable much used in biomedical applications [15, 16].

Moreover, in this study the potassium persulfate was also added to the cement, because it is an oxidizing agent that acts as a reaction initiator, and tetramethylethylenediamine (TEMED) as a reaction accelerator [17]. The polyethylene glycol diacrylate (PEG) was also added in this cement because it is a thermoplastic macromonomer, highly water soluble, has low immunogenicity and toxicity [18] and is capable of increasing the biocompatibility of nanoparticles.

Therefore, this study evaluated the addition of nano-hydroxyapatite, chitosan and potassium persulfate to the zinc oxide-magnesium (Zinc phosphate cement powder component), and the liquid phase composed of polyethylene glycol, TEMED and water to obtain the acidity control, to increase cytocompatibility and improve the antimicrobial activity of commercial zinc phosphate cement.

MATERIALS AND METHODS:

Materials: The polyethylene glycol diacrylate (PEG) (MW 10000 g mol^{-1}), chitosan low molecular weight (poly-D-glucosamine-deacetylated-chitin) 80% degree of deacetylation, and ultrapure deionized water were purchased from Sigma-Aldrich (São Paulo, SP, Brazil), and tetra-methylethylenediamine (TEMED)$(CH_3)_2NCH_2$ $CH_2N(CH_3)_2$, as polymerization accelerator from OmniPur (São Paulo, Brazil). Calcium nitrate ($Ca(NO_3)_2 \cdot 4H_2O$) (MW 164,08 g mol^{-1}), was purchased from LabSynth (São Paulo, Brazil) and sodium phosphate dibasic anhydrous (Na_2HPO_4) (MW 141.96) from Vetec, São Paulo, Brazil), Zinc oxide (90%) and Magnesium oxide (10%) (Zinc

phosphate powder from S.S. White-Rio de Janeiro, RJ, Brazil), potassium persulfate ($K_2S_2O_8$) (MW 270. 32 g mol^{-1}) from Schuchardt OHG Merck (Darmstadt, Germany).

Synthesis of Nano-hydroxyapatite: Nano-hydroxyapatite (nHA) was synthesized by a co-precipitation method. The materials used for this purpose were calcium nitrate and sodium phosphate dibasic anhydrous. The hydroxyapatite nano-particles less than 100 nm were synthesized using a chemical precipitation method [19]. According to this method, 6.5 g of $Ca(NO_3)_2 \cdot 4H_2O$ (0.04 M) and 4.3 g of Na_2HPO_4(0.030 M) were dissolved in 50 mL and 45 mL of deionized water, respectively. The pH of the reaction mixture was adjusted at 9–10 by adding NaOH solution. A white gelatinous precipitate formed was filtered, washed with deionized water. The washed precipitate of nHA was collected and kept in the oven at 85 °C overnight [19, 20].

Cement Preparation and Setting Times: The cement prepared consists of two phases: the solid and liquid phases were made according to the ISO 6876/2012 [21] standards with the modification of leaving the cement with a solid consistency to facilitate manipulation.

Table 1 showed the compositions of complete cement (HCP), the cement without nHA(CP), the cement without chitosan (HP), and the cement without zinc oxide-magnesium (CH).

TABLE 1: COMPOSITIONS OF POWDER AND LIQUID PHASES FROM EACH FORMULATION

Groups	Composition	Liquid phase
HCP	50 mg of hydroxyapatite nanoparticles (0.049 mol), 50 mg of zinc oxide-magnesium (0.129 mol), 50 mg of chitosan (low molecular weight), 50 mg potassium persulfate (0.184 mol).	1500 mg of the polyethylene glycol diacrylate (PEG) (10.000 Da), 140 mg of TEMED, and 1300 mg ultrapure deionized water
CP	50 mg of of zinc oxide-magnesium (0.129 mol), 50 mg of chitosan (low molecular weight), 50 mg potassium persulfate (0.184 mol).	
HP	50 mg of hydroxyapatite nanoparticles (0.049 mol), 50 mg of of zinc oxide-magnesium (0.129 mol), 50 mg potassium persulfate (0.184 mol).	
CH	50 mg of hydroxyapatite nanoparticles (0.049 mol), 50 mg of chitosan (low molecular weight), 50 mg potassium persulfate (0.184 mol).	

The liquid phase consisted of 1500mg of the polyethylene glycol diacrylate (PEG) (10.000 Da), 140mg of TEMED as accelerator of reaction, and 1300 mg ultrapure deionized water. The remainder was stored for further use. For the solid phase, all the cements use only 0.140 mL of the prepared liquid portion.

Determination of the cement setting time was performed according to Specification No. 57 of the American National Standard Institute/American Dental Association (ANSI/ADA/2000) [22], under controlled temperature conditions at 37 ± 1° C. The cement, previously spatulated, was inserted in molds of 10 mm diameter and 2 mm height. Ten specimens from each cement group were made and numbered from 1 to 10. After starting the spatulation, the samples were subjected to surface marking for the final prey. The time elapsed from the beginning of the spatulation to the moment when it was no longer possible to visualize any marking on the surface of the specimen, representing, respectively, the final setting time of the cement, the Zinc phosphate cement SSW® (CPZn) was tested as a control. The one-way ANOVA and Tukey's tests were used to compare the formulations.

Evaluation of the pH and Calcium Ion Released: The pH and calcium ion released were performed using molds measuring 2 mm high and 10 mm in diameter filled with the cement of each group (n = 10) weighing 180 mg each sample.

The groups were complete cement (HCP), the cement without nano-hydroxyapatite (CP), the cement without chitosan (HP), the cement without zinc oxide-magnesium (HC), and Zinc phosphate cement SSW® (CPZn) tested as a control.

Each specimen was immersed in flasks 10 mL of distilled water and kept in an oven at 37 °C throughout the experimental periods. They were removed from the flasks at each period, centrifuged and the supernatant collected. The experimental periods were 3, 12, and 24 h and 7, 14, and 21 days. The pH of the solutions was measured immediately after the end of each trial period using a pre-calibrated HI 221 Hanna Instruments pH meter.

Calcium ions released were measured on a Hilger & Watts H1170 atomic absorption spectrophotometer (Analytical Division, Rank Precision Industries Ltd., London, UK). The distilled water was aspirated into a chamber, mixed with acetylene and an oxidizer, and then burned (flame height = 5 cm). The released calcium (mg L^{-1}) from the materials was quantified using a hollow cathode lamp specifically for reading calcium data (wavelength = 422.7 nm and 0.7 nm window), operated at 20 mA. The calcium concentrations obtained were compared to a standard curve [23].

Scanning Electron Microscopy-Energy Dispersive Spectroscopy Analysis: The cement HCP, CP, HP, and HC after final setting time were analyzed by scanning electron microscopy (SEM; JEOL JSM, 6360LV) with energy dispersion spectroscopy (EDS) to determine the specific elements that comprise the sample. The percentage distribution of particles at the cement was calculated with digital image analysis software (Image J 1.60, Scion; Frederick, MD, USA) in a selected area on each image.

Thermal Analysis: The TG curves of the cement HCP, CP, HP, and HC were obtained on a Shimadzu DTG-60 thermobalance with an N_2 flow at 90 mL·min-1 and synthetic airflow at 20 $mL \cdot min^{-1}$. A heating program of 25 °C to 700 °C was used to analyze the complete cement samples, with a heating rate of 10 $^oC \cdot min^{-1}$. Each sample (5.00 ± 0.05 mg) was packaged in an alumina crucible. The graphs were analyzed using software Origin Pro 7.0 to characterize the weight loss.

Powder X-ray Diffraction Analysis: The X-ray powder diffraction patterns of the cement samples HCP, CP, HP, and HC were analyzed on an X-ray diffractometer (Shimadzu apparatus, XRD-7000 model), and the graphs were analyzed using software Origin Pro 7.0. To evaluate the chemical composition of the cement samples, a copper pipe and Cuk_α (α =1.54051) radiation were used, with the 2θ angle ranging from 4 to 70 degrees and a scan rate of $4\theta\ min^{-1}$.

Raman Spectroscopy Study: Raman spectra of the cement HCP, CP, HP, and HC were obtained by an FT-Raman spectrometer (RFS100 model, Bruker), allowing spectra of macroscopic areas with a diameter of approximately 20 mm, equipped with a Nd+3/YAG laser operating at 1064 nm, a Ge-diode detector cooled with liquid nitrogen, a spectral resolution of 4 cm^{-1}, 1024 spectra accumulations, and an average of 200 mW of laser power on the sample. The graphs were analyzed using software Origin Pro 7.0; of note, all spectra were obtained at least twice to guarantee no changes in intensity for each one of the samples.

Solubility Test: Samples with smaller dimension could be a viable alternative for testing the solubility of root filling materials; based on ADA23 specification 57/2000 [22], and ISO 6876/2012 [21], cylindrical molds measuring 2 mm high and 10 mm in diameter were fabricated and filled with the tested types of cement (n=10). A nylon thread was embedded in the fresh mixture of the cement, and another glass slide also covered by cellophane was placed over the mold. The set was pressed manually and stored in an oven at 37 °C for a period corresponding to three times the initial setting time of each material.

The test specimens were removed from the molds, weighed on a precision balance (OHAUS | Pioneer® PA Analytical Electronic Balance, USA), placed in plastic receptacles with lids and containing 10 mL of distilled water, and then suspended by nylon threads attached to the containers. The receptacles remained in the oven at 37 °C for seven days, at which time the test specimens were removed from the distilled water, dried and placed in a dehumidifying chamber. The mass was measured before and after immersion of the samples in distilled water, and every 24 h after that, until attaining mass stabilization [23]. The loss of mass was expressed as a percentage of the original mass. The tested groups were HCP (n = 10), CP (n = 10), HP (n = 10), HC (n = 10), all without change in the proportion of the liquid portion. The control was the cement Zinc phosphate SSW® (CPZn).

Contact Angle Measurement: Cylindrical specimens with 2 mm high and 10 mm diameter, weighing 180 mg, of the tested groups were prepared samples n=10 for each group. Cement were prepared for contact angle measurement using the SEO equipment, Model Phoenix Mini. The one-way ANOVA and Tukey's test was used to

compare the formulations to control. The tests were performed using a drop of MilliQ water deposited on the surfaces of the specimens (0.10 µL each drop). The angle between the contact surface and the drop was achieved through SEO software from Surface ware 9.

Shear Strength Test: The test was performed in standard equipment (Compact Force Gauge/ Statement of Product Conformance-Mecmesin), capable of performing low amplitude shear load measurements. Depending on the results obtained in the shear tests, fractures in the samples were classified as cohesive or mixed (cohesive and adhesive) shear stress (MPa), which was obtained using sheer force of rupture measured in the equipment and area of the fracture region of the test piece, measured in mm^2: T=F / A.

The tested groups were HCP (n= 10), CP (n= 10), HP (n = 10), HC (n = 10). The control was the Zinc phosphate SSW® cement (CPZn), with 1 mm × 10 mm size.

The measured shear strength of each specimen group, considered as independent variable for cement types, were analyzed by one-way analysis of variance (ANOVA), considering two groups: cohesive and mixed fractures.

Cytotoxicity Assay: The samples of types of cement were tested in sterile glass cylindrical molds, 1mm in diameter and 5mm in height weighing 10 mg in six replicates, as follows: HCP, CP, HP, HC, comparing them with 10 mg of the Zinc phosphate cement SSW® (CPZn), and positive control with medium and cells.

The 3T3-L1 cells (murine fibroblasts) were grown in high-glucose DMEM (12800, Gibco) supplemented with 10% fetal bovine serum (FBS) and 1% of a solution containing antibiotic/antimycotic (Cultilab, Campinas, SP, Brazil) and cultured in an incubator at 37 °C and 5% CO_2. The cells were trypsinized with 0.25% trypsin-EDTA solution (Sigma) after reaching 70–80% confluence. A total of 2.5×10^3 cells/mL were grown on a 96-well plate and were used for treatment with cement when the cells reached a confluence of approximately 60-70%. And as a positive control the cells and the medium.

The treatments lasted for 24 h, after which the assessment of cytotoxicity was conducted using the MTT colorimetric assay (Life Technologies), according to the manufacturer's recommendations. The absorbance values at 570 nm were measured by using a plate reader [9, 12]. For the analysis of the data, the tests of variance analysis (ANOVA) and Tukey's multiple comparison were applied.

Disk Diffusion Test: The agar diffusion method was used to assess an antimicrobial activity of the cement. Subcultures of bacterial strains *Aggregatibacter actinomycetemcomitans* (A.a) (ATCC 29522) were cultivated in Brain Heart Broth Infusion (BHI- Himedia Laboratories, LBS Marg, India) with 0.0005% hemin (Sigma-Aldrich, St. Louis, MO.) *Porphyromonas gingivalis* (P.g) (ATCC 33277), and *Fusobacterium nucleatum* (*F.n)* (ATCC 25586) were cultured in Brain Heart Broth Infusion with 0.0005% Hemin, 0.0001% menadione (HiMedia Laboratories), and 0.0002% horse blood. *Staphylococcus aureus* (S.a) (ATCC 29213) were cultured in Brain Heart Broth Infusion.

P.g and *F.n* were cultured under anaerobic conditions (90% N_2 and 10% CO_2) at 37 °C for 24 h, *S.a* was incubated in aerobiosis, and plates with A.a were incubated in microaerophilic conditions (5 % O_2, 10 % CO_2 and 85 % N_2) for 24 h [24]. To standardize inoculum for susceptibility assays colonies were suspended in BHI broth supplemented with 0.0005% hemin, to reach optical density (OD_{600}) and 0.08 of absorbance (equivalent $1 \cdot 10^8$ bacterial/mL). After that, 0.2 mL of each bacterial suspension was inoculated in the Mueller-Hinton (Himedia Laboratories, LBS Marg, India) agar with spread plate technique. Afterward, cylindrical discs 5 mm in diameter by 2 mm in height containing 50 mg of the material to be tested was placed on the Petri plates with the aid of sterile tweezers and incubated under appropriate conditions according to each strain. After this period, measurements of growth inhibition halos were made. The experiments were carried out in triplicates for each microbial species.

The test specimens tested were the group's HCP, CP, HP, HC, and Zinc phosphate cement SSW® (CPZn) was tested as a positive control.

The analysis of the diameters of the inhibition halos formed in the agar diffusion test as a function of the material tested in the direct contact test was performed using one-way ANOVA and Tukey's t-test.

RESULTS AND DISCUSSION:

Setting Time: Table 2 presents the setting time values found to each cement expressed on minutes (mean ± S.D.) evaluated in this work. The results for this parameter showed an average time of 5.5 minutes ± 0.18 for the complete cement, and the other groups have shown extended setting time compared to the HCP group.

TABLE 2: MEAN AND STANDARD DEVIATION VALUES AT SETTING TIME FOR EACHCEMENT EXPRESSED IN MINUTES

Groups of cement	Setting time (min)		
	n	Mean	SD
Complete cement (HCP)	1	5.5	±0.18
Without nHA (CP)	1	5.6	±0.26
Without chitosan (HP)	1	6.4	±0.15
Without zinc oxide-magnesium (HC)	1	6.8	±1.20
Zinc phosphate cement SSW® CPZn (control)	10	5.4	±0.70

Significant difference compared with the control group (p≥0.05)

The values of all compared groups were not significant, but all setting times of groups were appropriate to facilitate the insertion of the material on the location of the injury. It is well known that cement used in clinical practice should allow for an adequate manipulation time, a reasonable setting time, and an appropriate pH. In this study, the setting time of 5.5 min under controlled temperature conditions at 37 °C ± 1 °C was adequate to avoid excessive fluidity of the cement and compromise its clinical performance [22].

pH and Calcium Ion Release: In **Table 3**, the pH values for all groups were near to neutral pH and few changes in 14 days; the complete cement group (HCP) presented pH values of 7.4 in 3 h, 7.4 in 12 h, 7.3 in 24 h, 7.2 in 7 days and 7.1 in 14 days, whereas the group without the nano-hydroxyapatite (CP) showed the pH with values lower in all experimental times (7.0 in 3 h, 6.9 in 12 h, 6.8 in 24 h, 6.8 in 7 days and 6.6 in 14 days) showing the probable influence of nano-hydroxyapatite on the alkalinity of the cement. It can be observed that the cement control, Zinc phosphate cement SSW® presents pH acid values of compared to the other groups (Significance p≤0.05).

TABLE 3: MEAN AND STANDARD DEVIATION VALUES OF pH AT EACH TIME POINT: COMPLETE CEMENT (HCP), CEMENT WITHOUT NANO-HYDROXYAPATITE (CP), CEMENT WITHOUT CHITOSAN (HP), CEMENT WITHOUT ZINC OXIDE-MAGNESIUM (HC), AND ZINC PHOSPHATE CEMENT SSW® (CPZN) TESTED AS A CONTROL

		pH Values				
Groups	N	3 hours Mean ± SD	12 hours Mean ± SD	24 hours Mean ± SD	7 days Mean ± SD	14 days Mean ± SD
HCP	10	7.4 ± 0.25*	7.4 ± 0.33*	7.3 ± 0.39*	7.2 ± 0.42*	7.1 ± 0.41*
CP	10	7.0 ± 1.30*	6.9 ± 0.91*	6.8 ± 0.45	6.8 ± 0.86	6.6 ± 0.40
HP	10	7.2 ± 0.28*	7.2 ± 0.83*	7.2 ± 0.59*	7.1 ± 0.53*	7.0 ± 0.71*
HC	10	7.0 ± 0.16*	7.1 ± 0.72*	6.9 ± 0.89*	6.9 ± 0.48	6.7 ± 0.43
CPZn	10	5.2 ± 0.81	5.2 ± 0.16*	5.0 ± 0.57*	5.5 ± 0.13*	5.7 ± 1.08*

*Significant difference compared with the control group (p≤0.05)

The pH may vary during the hardening process will influence the tissue response to the cement; for example, acidic conditions tend to induce an aseptic inflammatory response in the surrounding tissues [25]. The pH value of the cement was proximate to neutral pH. The slightly neutral medium is necessary to decrease the inflammatory response and also to accelerate the deposition of apatite in a similar way as observed for bones. Also crucial for cell differentiation, spreading, proliferation, and fibroblast formation, thus facilitating the repair of any found defects [26, 27].

Table 4 shows the calcium release values (mg L^{-1}); the complete cement group (HCP) showed continuous release close to 10 mg L^{-1}, maintaining a balance on the release ratio. The group without nano-hydroxyapatite (CP) and Zinc phosphate cement SSW® (CPZn) did not show the release of calcium ions, and the group without chitosan (HP) presented greater inconstancy of release values, showing its mucoadhesive capacity of controlled release in the other groups.

TABLE 4: MEAN AND STANDARD DEVIATION VALUES OF CALCIUM RELEASE (mg L^{-1}) AT EACH TIME POINT: COMPLETE CEMENT (HCP), CEMENT WITHOUT NANO-HYDROXYAPATITE (CP), CEMENT WITHOUT CHITOSAN (HP), CEMENT WITHOUT ZINC OXIDE-MAGNESIUM (HC), AND ZINC PHOSPHATE CEMENT SSW® (CPZN) TESTED AS A CONTROL

Calcium release (mg L^{-1})						
Groups	**n**	**3 hours Mean ± SD**	**12 hours Mean ± SD**	**24 hours Mean ± SD**	**7 days Mean ± SD**	**14 days Mean ± SD**
HCP	10	10.5 ± 0.6	10.8 ± 0.6	10.4 ± 0.5	10.2 ± 0.7	9.8 ± 0.8
CP	10	0	0	0	0	0
HP	10	13.7 ± 1.2	12.6 ± 0.7	10.03 ± 0.6	7.5 ± 0.8	5.2 ± 0.6
HC	10	10.3 ± 0.8	10.0 ± 0.8	9.8 ± 0.6	9.9 ± 0.7	9.6 ± 0.4
CPZn	10	0	0	0	0	0

(Significance p≥0.05)

Table 4 confirms the values of calcium release (mg L^{-1}) in which the complete cement group presented good solubility and alkalizing capacity on the surrounding medium. This alkalization promotes the formation of a calcium hydrate matrix [1], which has the potential to stimulate mineral deposition when it comes into contact with biological fluids, such as fluid dentine. Therefore, the chemical characteristics of the cement upon hydration lead to a bioactive surface that can help dentin repair, stimulating the mineralization of tissues [28, 29].

Therefore, the release of calcium and hydroxyl ions by the material favors the participation of these ions in the repair process. The Calcium ions react with tissue carbon dioxide, forming calcium carbonate that favors the proliferation of fibroblasts of the dental pulp, contributing to repair process [30].

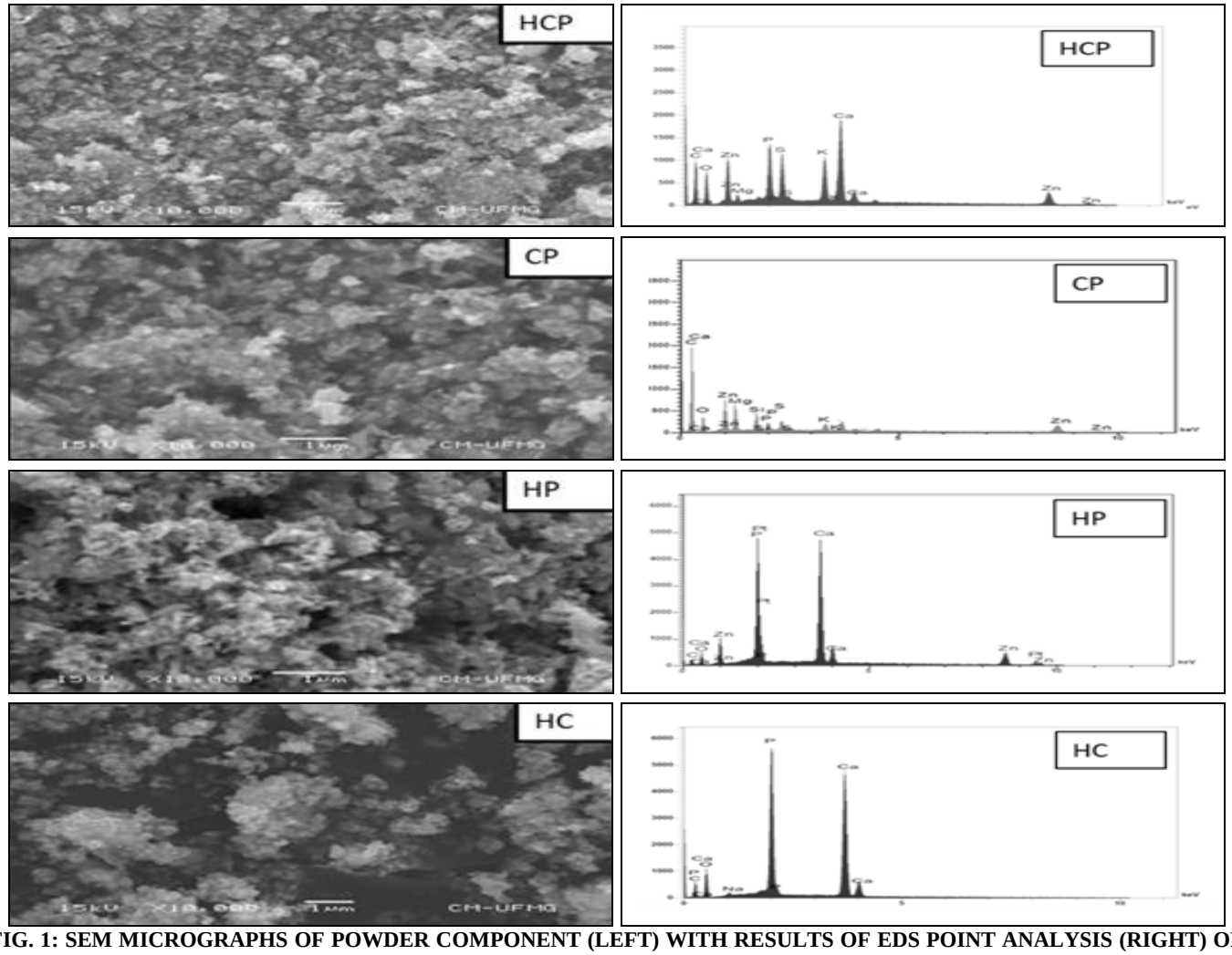

FIG. 1: SEM MICROGRAPHS OF POWDER COMPONENT (LEFT) WITH RESULTS OF EDS POINT ANALYSIS (RIGHT) OF SURFACE MORPHOLOGY THE CEMENT (HCP), CEMENT WITHOUT NANO-HYDROXYAPATITE (CP), CEMENT WITHOUT CHITOSAN (HP), CEMENT WITHOUT ZINC OXIDE-MAGNESIUM (HC), RESPECTIVELY. 10000 X

Scanning Electron Microscopy-Energy Dispersive Spectroscopy: The SEM revealed in the group's HCP, HP and HC some hydroxyapatite crystals in prismatic form **Fig. 1**; however, the majority of the calcium and phosphate crystals were rounded, according to the images obtained with increases from 10000×, and the EDS verified the presence of zinc and potassium bands as well as the presence of calcium and phosphate ions in a ratio of 1.67 belonging to the apatite, confirming this predominant chemical interaction in the cement of groups HCP, HC and HP. In the study, it was observed that the particles were uniformly dispersed in the cement surface.

The elemental analysis of the HCP, CP and HP reveals that some Mg was incorporated into the zinc structure. The powder of the HCP is largely composed of the round-shaped ZnO particles. Based on the results of EDS and SEM analyses, it's confirmed that the significant substances in the obtained powder were calcium, phosphate, and zinc, confirming this predominant chemical Zn interaction with nHA in the cement **Fig. 1**.

The variable morphology of cement particles in the composite, such as crystals prismatic [31]. Because of the small atomic mass, element (H) could not be manifested, and the appearance of the C was due to the application of conductive carbon paint. Since the cement was non-conducting, the utilization of metal spraying processing resulted in the emergence of Si [32].

Thermogravimetry: The thermogravimetry analyses of the complete cement HCP sample showed a weight loss when it was heated from 100 °C to 400 °C; such loss is related to the degradation of the organic components. At 700 °C, a final residue corresponding to 63% of the initial mass resulted, thus confirming the thermal stability of the hydroxyapatite residue **Fig. 2**.

According to the thermogravimetric analysis, the hydroxyapatite remained thermally stable as determined by the presence of residue even at 700 °C **Fig. 2**. This thermal stability could be responsible for the biological activity of the cement surface to induce tooth integration, as reported by others [33, 34]. Furthermore, it was evident that after the thermogravimetry test at 700°C, Zn particles and nHA were chemically compatible without interfering with the other's crystalline structure and stability [32].

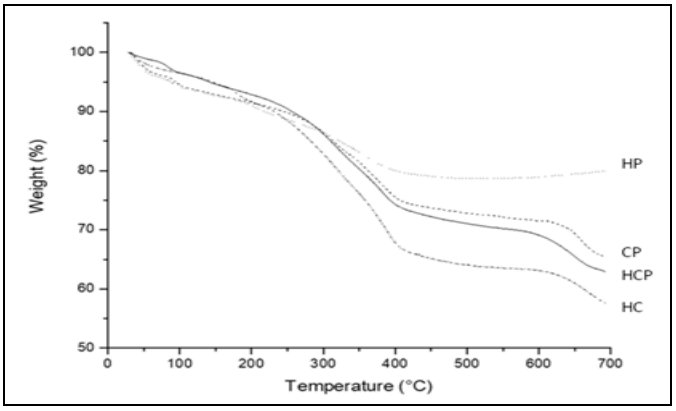

FIG. 2: THE THERMOGRAVIMETRIC CURVES OF THE CEMENT TESTED: COMPLETE CEMENT (HCP), CEMENT WITHOUT NANO-HYDROXYAPATITE (CP), CEMENT WITHOUT CHITOSAN (HP), AND CEMENT WITHOUT ZINC OXIDE-MAGNESIUM (HC)

X-ray Diffraction: Through the comparative analysis of the X-ray pattern of the cement the characteristic peaks of nano-hydroxyapatite and zinc oxide in the samples are verified. The main XRD reflection groups can be used to characterize nHA; one at 2θ = 36.0 ° and 49.5° the other group is ranging from 2θ = 31.1° to 2θ = 32.9°. However, the crystallographic profile of zinc oxide in groups of 2θ values is also 31.1 ° and 34.4°. The results of the group without zinc oxide-magnesium (HC) showed that there was a probable amorphization of the characteristic peaks, especially of nHA, evidencing the importance of the association of these structures [13].

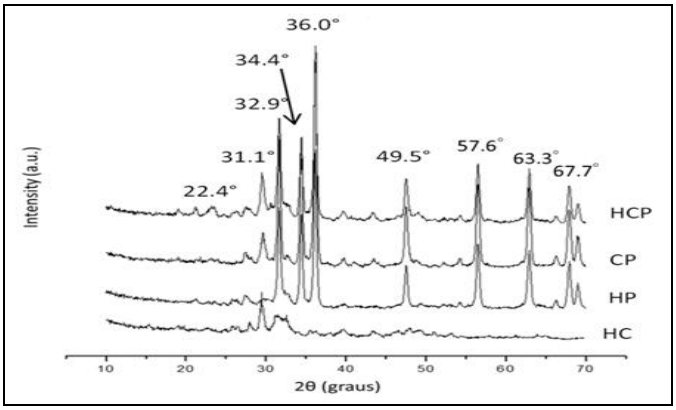

FIG. 3: X- RAY DIFFRACTOGRAM OF THE CEMENT TESTED SHOWING HIGH-INTENSITY PEAKS IN THE REGION AROUND 10–70/2Θ, OF COMPLETE CEMENT (HCP), CEMENT WITHOUT NANO-HYDROXYAPATITE (CP), CEMENT WITHOUT CHITOSAN (HP), AND CEMENT WITHOUT ZINC OXIDE-MAGNESIUM (HC)

The chitosan showed the characteristic peak at 2θ= 22.4°, which are typical fingerprints of semi-crystalline chitosan **Fig. 3**. The chitosan crystallinity is associated with a large number of hydroxide and amine groups present in its structure. These groups can form stronger intramolecular hydrogen bonds that lead to the regularity of the chitosan structure [35].

Raman Spectroscopy: In addition, the Raman spectrum of the cement showed the mapping of the cement interdiffusion zone, based on the presence of a band at 2781 cm^{-1} assigned to a C-H stretching mode from the PEG composing the liquid phase, another band, such as the one at 1453 cm^{-1} assigned to the C-H deformation mode from the PEG, was also present in the spectrum [36], thus characterizing the main components, impregnation of potassium persulfate was observed in the band 1086 cm^{-1} (symmetric stretching C-O of the group CO_3^{-2}. The intense band at 960 cm^{-1} was assigned as the main vibrational mode of phosphate of hydroxyapatite (the symmetric stretching mode of the PO_4 ion), whereas other specific bands, at 585 cm^{-1} (assigned to two O-P-O modes of the composite) were also observed in groups HCP, HC and HP. Another essential marker band at 1077cm^{-1} was assigned to the asymmetric axial deformation of C-O-C from the chitosan present in the composite structure except for group HP. The bands obtained in low-intensity peaks with magnesium oxide are at 1340 and 1568 cm^{-1}, in the groups. From the obtained spectrum, it was not possible to observe any specific bands characteristic for zinc oxide **Fig. 4**.

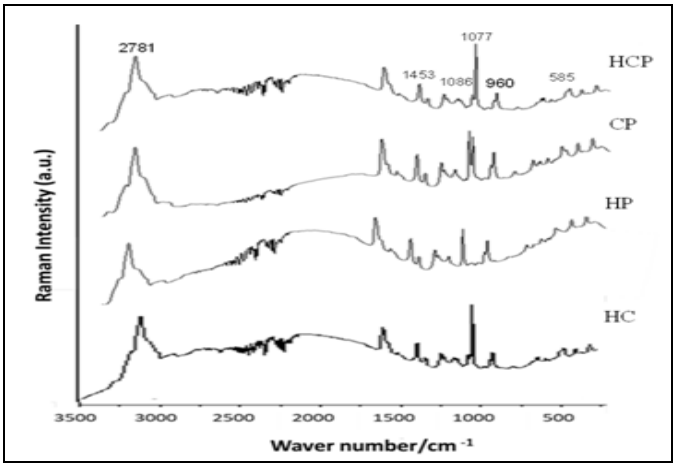

FIG. 4: FT-RAMAN SPECTERS OF THE CEMENT: COMPLETE CEMENT (HCP), CEMENT WITHOUT NANO-HYDROXYAPATITE (CP), CEMENT WITHOUT CHITOSAN (HP), AND CEMENT WITHOUT ZINC OXIDE-MAGNESIUM (HC)

Contact Angle: The contact angle measurements for the cement samples are presented on **Table 5**. These results were obtained by mean of the initial values of the first captured image of the drop-in contact with the specimen [26].

The results indicated smaller values of the angle for the complete cement than those the control cement, but the small difference indicated high water wettability of the cement.

TABLE 5: THE CONTACT ANGLE OF COMPLETE CEMENT (HCP), CEMENT WITHOUT NANO-HYDROXY-APATITE (CP), CEMENT WITHOUT CHITOSAN (HP), CEMENT WITHOUT ZINC OXIDE-MAGNESIUM (HC) AND CEMENT CONTROL (CPZN)

Groups	Contact angle (°)			
	n	Mean	SD	p-value
HCP	10	23.27	±0.425	< 0.001
CP	10	22.06	±0.608	0.04
HP	10	22.48	±0.808	0.05
HC	10	16.18	±0.526	< 0.01
CPZn	10	28.945	±1.82	

p-value- Significant difference compared with the control group

The values of the contact angle measurements for the complete cement and the control cement indicated smaller values of the angle for the complete cement than those for the control cement, but the difference was small, indicating high water wettability [37] of experimental cement. This is expected to occur because control cement, which is standard cement, normally shows a hydrophobic surface slightly more increased than cement with new compositions and treatments.

The more hydrophilic (contact angle < 90 °) the surface, the higher the probability of hydrogen bonding, while hydrophobic substances (contact angle > 90°) tend to interact with each other and also through Van der Waals bonds (low hydrogen bonding capability) **Table 5**. A hydrophobic surface is more prone to bacterial adhesion [38].

Solubility: Table 6 shows the means and standard deviations of the solubility percentage of the types of cement studied. Most of the cement had a solubility below the maximum recommended by ADA standards 57 [22] and ISO 6876/2012 [21], which is 3%. All the cement evaluated presented low solubility and did not differ statistically among one another ($p \geq 0.05$).

TABLE 6: PERCENTAGE OF SOLUBILITY VALUES OF THE CEMENT STUDIED: CEMENT COMPLETE (HCP), CEMENT WITHOUT NANO-HYDROXYAPATITE (CP), CEMENT WITHOUT CHITOSAN (HP), CEMENT WITHOUT ZINC OXIDE-MAGNESIUM (HC) AND THE CONTROL CEMENT ZINC PHOSPHATE SSW® (CPZN)

Groups (n=10)	Solubility (%)
HCP	2.15 ± 0.037
CP	1.98± 0,094
HP	1.65 ± 0.18
HC	1.93 ± 0.19
CPZn	1.65 ± 0.10

(Significance p≥0.05)

The stimulation to the mineralization process may be associated with the solubility presented in the cement through alkalinization and the release of calcium ions [39]. However, the solubility of material must follow norms since high solubilization can lead to empty spaces, compromising the sealing obtained.

In the present study, the cement presented solubility in **Table 6**, with an average value of 2.15%, near the determined limit of the standards by ADA standards 57 [22] and ISO 6876/2012 [21]. This fact may explain the higher release of calcium ions and the high pH observed for the material and hydrophilicity given by the contact angle because high solubility values may be related to rapid drug release and marginal infiltration, compromising its clinical effectiveness [40].

Shear Strength: The results of shear strength tests for cement are presented in **Table 7**. Due to the different morphology of fractures presented in the tests, the table presents the values for shear strength according to two types of fracture: cohesive and mixed fractures. The results indicate a predominance of cohesive fractures for the control cement (CPZn), whereas for complete cement (HCP) the occurrence of mixed fractures was greater, being surpassed only by the cement without zinc oxide-magnesium (HC). These results would be related to the porous structure of this cement, which causes a higher incidence of propagation of mixed fractures along with the sample and higher variations in the results [41]. All test values presented the statistical significance of results (p ≤0.05).

TABLE 7: SHEAR STRENGTH OF CEMENT COMPLETE (HCP), CEMENT WITHOUT NANO-HYDROXYAPATITE (CP), CEMENT WITHOUT CHITOSAN (HP), CEMENT WITHOUT ZINC OXIDE-MAGNESIUM (HC) AND THE CONTROL CEMENT ZINC PHOSPHATE SSW® (CPZN)

Groups	Shear strength (MPa)					
	Fracture		Mean	SD	Range (min–max)	
HCP (n=10)	Cohesive	7	4.544	±0.53	3.793 – 5.705	< 0.001
	Mixed	3	7.542	±0.42	7.133 – 8.264	
CP (n=10)	Cohesive	8	4.684	±0.61	3.576– 5.421	0.04
	Mixed	2	6.712	±0.67	6.138 – 8.002	
HP (n=10)	Cohesive	10	4.776	±0.34	3.981 – 5.976	0
	Mixed	0	0	0	0	
HC (n=10)	Cohesive	6	3.324	±0.25	3.102 – 5.403	0.05
	Mixed	4	4.345	±0.56	4.003 – 5.76	
CPZn (n=10)	Cohesive	8	6.76	± 0.66	5.29 – 7.24	
	Mixed	2	10.08	± 0.08	10 – 10.17	

In relation to the results found for shear strength indicate a predominance of cohesive fractures for the control cement, whereas for complete cement (HCP) the occurrence of mixed fractures was large, however, not surpassing the cement without zinc oxide-magnesium (HC), showing that the zinc oxide-magnesium in its composition is important to improve the mechanical strength of the cement.

These results would be related to the porous structure of this cement, which causes a higher incidence of propagation of mixed fractures along the sample and higher variations in the results.

Cytotoxicity: Fig. 5 represents the cell viability test performed with the complete cement as well as cement without nano-hydroxyapatite in its composition, without zinc oxide-magnesium, without chitosan, and cells without treatment (positive control). When evaluated the cytotoxicity, it was verified that 3T3 fibroblasts after 24 h of treatment with the complete cement group showed that 79.24% cell viability. However, the samples without nano-hydroxyapatite (CP) or without chitosan (HP) showed cytotoxicity as the cell viabilities were 66.23% and 65.62%, respectively, and the phosphate zinc (CPZn) presented viability of 69.98%.

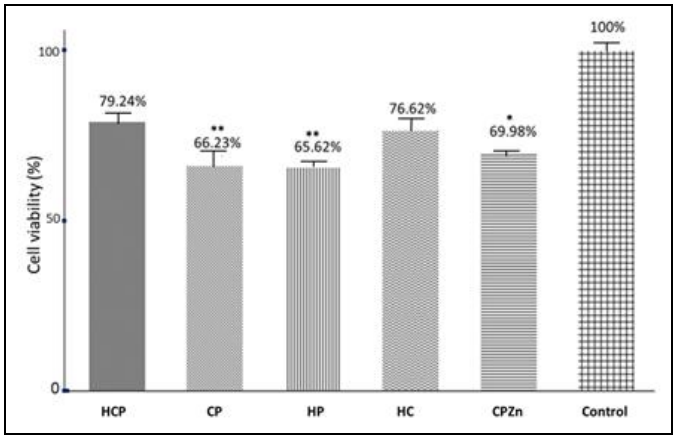

FIG. 5: CELL VIABILITY OF 3T3 FIBROBLASTS TREATED WITH THE CEMENT TESTED: COMPLETE CEMENT (HCP), CEMENT WITHOUT NANO-HYDROXYAPATITE (CP), CEMENT WITHOUT CHITOSAN (HP), CEMENT WITHOUT ZINC OXIDE-MAGNESIUM (HC) OVER 24 h (MEAN AND STANDARD DEVIATION OF TREATMENTS; ** P<0.01 IN RELATION TO THE CONTROL; * P <0.05 COMPARED TO THE CONTROL

The group's CP and HP presented a statistically significant difference in relation to the positive control ($p < 0.010$) and the negative control (CPZn) indicated a significant difference ($p<0.05$) in relation to the positive control. Since the complete cement-treated cells showed 79.24% cell viability, there was no considerable cytotoxicity **Fig. 5**. The physicochemical properties and the biocompatibility, of the cement were satisfactory [12, 42] to maintain the necessary conditions the material comes in contact with dental tissues in a way to replace the acid reaction of the commercial cement.

Antimicrobial Activity: The results of the halos of inhibition on agar diffusion test with the microorganisms *S.a*, *P.g*, *F.n*, and *A.a* are shown at **Table 8**. The level of significance for all tests was $p \leq 0.05$ at regarding the control.

Table 8: MEAN DIAMETERS AND STANDARD DEVIATION VALUES OF HALOS OF INHIBITION: COMPLETE CEMENT (HCP), CEMENT WITHOUT NANO-HYDROXYAPATITE (CP), CEMENT WITHOUT CHITOSAN (HP), CEMENT WITHOUT ZINC OXIDE-MAGNESIUM (HC), AND ZINC PHOSPHATE CEMENT SSW® (CPZN) TESTED AS A CONTROL ON *P. GINGIVALIS* (*Pg*), *F. NUCLEATUM* (*Fn*), *S. AUREUS* (*Sa*) AND *A. ACTINOMYCETEMCOMITANS* (*Aa*) IN THE AGAR DIFFUSION TEST

	Halos of inhibition (mm)				
Bacterial Strain (n=3)	**HCP Mean/SD**	**CP Mean/SD**	**HP Mean/SD**	**HC Mean/SD**	**CPZn Mean/SD**
Pg	28.0 ±0.4*	22.1± 1.0*	20.0 ± 0.8*	19.3 ±1.2*	16.0 ± 0.8
Fn	24.5 ±1.4*	21.3± 1.2*	19.1 ±0.6	18.4 ±0.4	18.0 ± 0.7
Sa	24.0±0.9*	18.3± 0.4*	23.3±3.0*	22.0 ±1.4*	18.6 ± 0.4
Aa	20.3±1.8*	16.3 ± 0.4*	17.0±1.4*	20.3±0.4*	18.0 ± 0.8

* Significant difference compared with the control group ($p \leq 0.05$)

The antimicrobial tests carried out by the agar diffusion method against *P.g*, *F.n*, *S.a* and *A.a* showed inhibitory activity higher for complete cement (24.1 mm ± 3.1), (28.0 ± 0.4), (24.5 ± 1.4) and (24.0 ± 0.9), respectively, than cement control (16.0 ± 0.8), (18.0 ± 0.7), (18.6 ± 0.4) and (18.0 ± 0.8) with $p \leq 0.05$. It is observed that the *P. g* strain presented larger inhibitions (28.0 mm) over other bacteria tested, and it is also observed that the cement HCP presented the largest inhibition halos compared with the other materials tested on all the bacteria, including Zinc phosphate cement used as a control.

Microorganisms are responsible for the etiopathogenesis of the main pulpal and periapical alterations [43], as well as the primary causative agents that act on the secondary complicating agents in the process of tissue healing. Considering this role of infections can be considered, control and elimination of the microorganisms present in the pulp cavity [44]. A study was made of the antimicrobial capacity of dental cement in bacterial cultures of *S. mutans*, *S. pyogenes*, *S.aureus*, *E. faecalis*, and *E. coli* showed that Zinc phosphate cement (CPZn) produced inhibition halos on S. *pyogenes*, S. *mutans*, and *S. aureus* microorganisms [45]. The present study showed that the cement inhibited *S.a*, *P.g*, *F.n*, *A.a* with larger halos and antimicrobial activity than those of Zinc phosphate cement (CPZn). The inhibition zone of the cement was more potent for all strains. **Table 8,** confirming that the addition of all components provides a desired antimicrobial action.

CONCLUSION: In conclusion, the addition of both chitosan and nano-hydroxyapatitetozinc oxide-magnesium was an excellent strategy to produce dental cement with similar physicochemical properties of Zinc phosphate cement, at the same time exhibiting high cytocompatibility, maintaining its resistance and

antimicrobial action. Most importantly, the cement opens the possibility of obtaining a more compatible material for use in clinical settings, and its biological properties should be considered before further *in-vivo* tests.

ACKNOWLEDGEMENT: The authors would like to thank INCT (National Institute of Science and Technology Nanobiofar) and CNPq, the Center of Microscopy at the Universidade Federal de Minas Geraisfor assistance, Capes (Coordenação de Aperfeiçoamento de Pessoal de Nível Superior), and FAPEMIG (Fundação de Amparo à Pesquisa do Estado de Minas Gerais).

CONFLICTS OF INTEREST: The authors declare that they have no conflict of interest.

FUNDING: This work was supported by Foundation for Research Support of the State of Minas Gerais (FAPEMIG) APQ-01982-16, Brazil, CNPq 308942/2016-7, Capes 88882.348761/2019-01; and Pró- reitoria de Pesquisa (PRPq) of Universidade Federal de Minas Gerais, Brazil.

REFERENCES:

1. Altaii M, Richards L and Rossi-Fedele G: Histological assessment of regenerative endodontic treatment in animal studies with different scaffolds: A systematic review. Dental Traumatology 2017; 33(4): 235-44.
2. Toledano M, Muñoz-Soto E, Aguilera FS, Osorio E, González-Rodríguez MP, Pérez-Álvarez MC, Toledano-Osorio M and Osorio R: A zinc oxide-modified hydroxyapatite-based cement favored sealingability in endodontically treated teeth. Journal of Dentistry 2019; 88: 103-62.
3. Imura K, Hashimoto Y, Okada M, Yoshikawa K and Yamamoto K: Application of hydroxyapatite nanoparticle-assembled powder using basic fibroblast growth factor as a pulp-capping agent. Dental Material Journal 2019; 38(5): 713-20.
4. Portella FF, Collares FM, Santos PD, Sartori C, Wegner E, Leitune VC and Samuel SM: Glycerol Salicylate-based Pulp-Capping Material Containing Portland Cement. Brazil Dental Journal 2015; 26(4): 357-62.
5. Basaran ET and Gokce Y: Evaluation of the influence of various restoration techniques on fracture resistance of endodontically treated teeth with different cavity wall thicknesses. Nigerian Journal of Clinical Practice 2019; 22(3): 328-34.
6. Kaur M, Singh H, Dhillon JS, Batra M and Saini M: MTA versus biodentine: review of literature with a comparative analysis. Journal of Clinical and Diagnostic Research 2017; 11(8): 01-5.
7. Suzuki M, Taira Y, Kato C, Shinkai K and Katoh Y: Histological evaluation of direct pulp capping of rat pulp with experimentally developed low-viscosity adhesives containing reparative dentin-promoting agents. Journal of Dentistry 2016; 44: 27-36.
8. Zancan RF, Cavenago BC, Oda DF, Bramante CM, Andrade FB and Duarte MAH: Antimicrobial activity and physicochemical properties of antibiotic pastes used in regenerative endodontics. Brazil Dental Journal 2019; 30(6): 536-41.
9. Abo El-Mal EO, Abu-Seida AM and El Ashry SH: A comparative study of the physicochemical properties of hesperidin, MTA-Angelus and calcium hydroxide as pulp capping materials. Saudi Dental Journal 2019; 31(2): 219-27.
10. AlZain SA: Effect of home bleaching on surface of zinc phosphate cement: A scanning electron microscopic study. Nigerian Journal of Clinical Practice2018; 21(6): 807-11.
11. Jun SK, Kim HW, Lee HH and Lee JH: Zirconia-incorporated zinc oxide eugenol has improved mechanical properties and cytocompatibility with human dental pulp stem cells. Dental Material 2018; 34(1): 132-42.
12. Li Z, Yubao L, Yi Z, Lan W and Jansen JA: *In-vitro* and *in-vivo* evaluation on the bioactivity of ZnO containing nano-hydroxyapatite/chitosan cement. Journal of Biomedical Materials Research Part A 2010; 93(1): 269-79.
13. Fang CH, Lin YW, Lin FH, Sun JS, Chao YH, Lin HY and Chang ZC: Biomimetic Synthesis of Nanocrystalline Hydroxyapatite Composites: Therapeutic Potential and Effects on Bone Regeneration. International Journal of Molecular Sciences 2019; 20 (23): 1422-37.
14. Delgado JA, Alonso LM, Nascimento J, Macedo KP, Ribeiro AA, Oliveira MV, Alfonso A, Martinez S and García-Vallès M: Sintering Behavior of Nanostructured Hydroxyapatite Ceramics. Key Engineering Materials 2015; 631: 207-211.
15. Yusof NAA, Zain NM and Pauzi N: Synthesis of ZnO nanoparticles with chitosan as stabilizing agent and their antibacterial properties against Gram-positive and Gram-negative bacteria. International Journal of Biological Macromolecules 2019; 124: 1132-6.
16. Vaz JM, Pezzoli D, Chevallier P, Campelo CS, Candiani G and Mantovani D: Antibacterial coatings based on chitosan for pharmaceutical and biomedical applications. Curr Pharm Des 2018; 24(8): 866-85.
17. Shih CH, Trong-Ming D and Wen-Yen C: Free radical degradation of chitosan with potassium persulfate. Polymer Degradation and Stability 2002; 75(1): 73-83.
18. Khor E, Guo CM, Wu H and Lim LY, 2011: Bone and / or dental cement composition and uses thereof. US Patent 20110136935 A1, Jun 9.
19. Chung JH , Kim YK, Kim K, Kwon TY, Vaezmomeni SZ, Samiei M, Aghazadeh M, Davaran S, Mahkam M, Asadi G and Akbarzadeh A: Synthesis, characterization, biocompatibility of hydroxyapatite–natural polymers nanocomposites for dentistry applications. Artif Cells Nanomed Biotechnol 2014; 44: 277-84.
20. Andharipande SL and Sondawale SS: Review on Synthesis of Hydroxyapatite and its Bio-composites. International Journal of Science Engineering and Technology Research 2016; 05: 3410-3416.
21. ISO 6876/2012 International Organization for Standardization. Dental Root Canal Sealing Materials.Geneve.
22. ANSI/ADA (2000) Specification no. 57: endodontic sealing materials. Chicago, IL: ANSI/ADA.
23. Bosso-Martelo R, Guerreiro-Tanomaru JM, Viapiana R, Berbert FLCV, Basso Bernardi MI and Tanomaru-Filho M: Physicochemical properties of calcium silicate cements associated with microparticulate and nanoparticulate

radiopacifiers. Clinical Oral Investigations 2016; 20(1): 83-90.
24. Deck MK, Anderson ES, Buckner RJ, Colasante G, Coull JM, Crystal B, Latta PD, Fuchs M, Fuller D, Harris W, Hazen K, Klimas LL, Lindao D, Meltzer MC, Morgan M, Shepard J, Stevens S, Wu F and Fiandaca MJ: Multicenter evaluation of the Staphylococcus Quick FISH method for simultaneous identification of *Staphylococcus aureus* and coagulase-negative staphylococci directly from blood culture bottles in less than 30 minutes. Journal of Clinical Microbiology 2012; 50(6): 1994-8.
25. Anusavice KJ: Phillips Dental Materials, twelfth ed. Elsevier, Rio de Janeiro 2013.
26. Preoteasa CT, Sultan AN, Popa L, Ionescu E, Iosif L and Ghica MV: Wettability of some dental materials. Optoelectronic Advan Mater Communic 2011; 5(8): 874 - 8.
27. Asghari-Sana F, Çapkın-Yurtsever M, Kaynak-Bayrak G, Tunçay E, Kiremitçi AS and Gümüşderelioğlu M: Spreading, proliferation and differentiation of human dental pulp stem cells on chitosan scaffolds immobilized with RGD or fibronectin. Cytotechnology 2017; 69(4): 617-30.
28. Faraoni G, Finger MS, Masson MC and Victorino FR: Comparative assessment of flow and setting time of the MTA Fillapex ™ sealer. RFO 2013; 18: 180-4.
29. Jagtap P, Shetty R, Agarwalla A, Wani P, Bhargava K and Martande S: comparative evaluation of cytotoxicity of root canal sealers on cultured human periodontal fibroblasts: *in-vitro* study. The Journal of Contemporary Dental Practice 2018; 19(7): 847-52.
30. Swarup SJ, Rao A, Boaz K, Srikant N and Shenoy R: Pulpal response to nano hydroxyapatite, mineral trioxide aggregate and calcium hydroxide when used as a direct pulp capping agent: an *in-vivo* study. Journal of Clinical Pediatric Dentistry 2014; 38(3): 201-6.
31. Lin JF, Liu WY, Zhang WY, Chen QH, Yuan YB, Yang LD, Xiao YH and Li MQ: The effect of modification of hydroxyapatite whisker with zinc acetate *via* sol–gel technology. Applied Mechanics and Materials 2013; 364: 655-9.
32. Yu J, Zhang W, Li Y, Wang G, Yang L, Jin J, Chen Q and Huang M: Synthesis, characterization , antimicrobial activity and mechanism of a novel hydroxyapatite whisker / nano zinc oxide biomaterial. Biomedical Materials 2015; 10: 15001-14.
33. Menezes M, Prado M, Gomes B, Gusman H and Simão R: Effect of photodynamic therapy and non-thermal plasma on root canal filling: analysis of adhesion and sealer penetration J of Applied Oral Sci 2017; 25(4): 396-403.
34. Quintana RM, Jardine AP, Grechi TR, Grazziotin-Soares R, Ardenghi DM, Scarparo RK, Grecca FS and Kopper PMP: Bone tissue reaction, setting time, solubility, and pH of root repair materials. Clinical Oral Investigations 2019; 23(3): 1359-66.
35. Muhammad S, Tariq Y and Muhammad AR: Structural, Thermal, and Antibacterial Properties of Chitosan/ZnO. Polymer Composites 2014; 35(79).
36. Di Foggia M, Prati C, Gandolfi MG and Taddei P: Spectroscopic and morphological data assessing the apatite forming ability of calcium hydroxide-releasing materials for pulp capping. Data in Brief 2019; 23: 103719.
37. Liu F, Shi Z and Dong Y: Improved wettability and interfacial adhesion in carbon fibre/epoxy composites via an aqueous epoxy sizing agent. Composites Part A 2018; 112: 337-45.
38. De-la-Pinta I, Cobos M, Ibarretxe J, Montoya E, Eraso E, Guraya T and Quindós G: Effect of biomaterials hydrophobicity and roughness on biofilm development: Journal of Materials Science: Materials in Medicine 2019; 30(7): 77.
39. Pushpa S, Maheshwari C, Maheshwari G, Sridevi N, Duggal P and Ahuja P: Effect of pH on solubility of white Mineral Trioxide Aggregate and Biodentine: An *in-vitro* study. Journal of Dental Research, Dental Clinics, Dental Prospects 2018; 12(3): 201-7.
40. Peralta SL, Leles SB, Dutra AL, Guimarães VBDS, Piva E and Lund RG: Evaluation of physical-mechanical properties, antibacterial effect, and cytotoxicity of temporary restorative materials. Journal of Applied Oral Science 2018; 26:e20170562.
41. Lezaja MJBM, Veljovic DN and Miletic V: Shear bond strength to dentine of dental adhesives containing hydroxyapatite nano-fillers. Journal of Adhesion Science and Technology 2016; 30(24): 2678-89.
42. Esteban-Tejeda L, Smirnov A, Prado C, Moya JS, Torrecillas R and Bartolomé JF: Multifunctional ceramic-metal biocomposites with Zinc containing antimicrobial glass coatings. Ceramic International 2016; 42: 7023-29.
43. Chen WP, Chang SH, Tang CY, Liou ML, Tsai SJ and Lin YL: Composition Analysis and Feature Selection of the Oral Microbiota Associated with Periodontal Disease. BioMed Research International 2018; 3130607.
44. Pereira RS, Rodrigues VAA, Furtado WT, Gueiros S, Pereira GS and Avila-Campos MJ: Microbial analysis of root canal and periradicular lesion associated to teeth with endodontic failure. Anaerobe 2017; 48: 12-8.
45. Domon H, Hiyoshi T, Maekawa T, Yonezawa D, Tamura H, Kawabata S, Yanagihara, K.Kimura O, Kunitomo E, and Terao Y: Antibacterial activity of hinokitiol against both antibiotic-resistant and -susceptible pathogenic bacteria that predominate in the oral cavity and upper airways. Microbiology and Immunology 2019; 63(6): 213-22.

How to cite this article:
Paula GC, Trajano A, Pinzón-García AD, Sinisterra RD and Cortes ME: Increased properties and citocompatibility of zinc oxide-magnesium cement. Int J Pharm Sci & Res 2020; 11(11): 5484-96. doi: 10.13040/IJPSR.0975-8232.11(11).5484-96.